The nature of bonding in pericyclic and pseudopericyclic transition states: Thermal chelotropic decarbonylations

ARTICLE *in* THE JOURNAL OF CHEMICAL PHYSICS · MAY 2003

Impact Factor: 2.95 · DOI: 10.1063/1.1566740

1 AUTHOR:

Eduardo Chamorro
Universidad Andrés Bello
79 PUBLICATIONS **1,690** CITATIONS

SEE PROFILE

The nature of bonding in pericyclic and pseudopericyclic transition states: Thermal chelotropic decarbonylations

E. Chamorro[a)]
Departamento de Ciencias Químicas, Facultad de Ecología y Recursos Naturales, Universidad Andrés Bello, República 217, Santiago, Chile

(Received 6 February 2003; accepted 19 February 2003)

The electron localization function (ELF), a local measure of the Pauli repulsion, is shown like a useful descriptor of bonding at pericyclic and pseudopericyclic transition states. The main differences between these two relevant topologies have been investigated in detail through the examination of well-characterized typical allowed-symmetry thermal decarbonylations. It is shown that results based on the electron fluctuation between the ELF basin populations at the reaction center, provides a consistent description of bonding which complements the traditional Woodward–Hoffmann symmetry-orbital based analysis. © *2003 American Institute of Physics.*
[DOI: 10.1063/1.1566740]

I. INTRODUCTION

Primary and/or secondary interactions between orbitals have been usually invoked and applied in order to understand the reaction mechanism of pericyclic and pseudopericyclic processes.[1–11] In this context, it has been pointed out that the fundamental difference among these two topologies is the conservation or not of a cyclic orbital overlap between the orbitals involved in bonding changes at the transition state. Henceforth, the lack of orbital overlap in a pseudopericyclic reaction has significant implications in the global (i.e., thermodynamic) and local (i.e., selectivity) chemistry of these systems. The interpretation of the mechanism of electrocyclization of (*Z*)-1,2,4,6-heptatetraene and its heterosubstituted analogs,[1] the reactions of conjugated ketenes with formaldimine,[2] the diasteroselectivity and reactivity of oxoketene and imidoylketene,[3] the antiaromaticity character of transition state in the conversion of *N*-acyl-4-acyloxy-β-lactams into 2-substituted 1,3-oxazin-6-ones,[4] the reactions of camphorketene,[5] the base-catalyzed bicyclic Boulton–Katritzky rearrangement,[6] the thermal cyclization of $(2Z)$-hexa-2,4,5-trienals and their Schiff bases,[7] the electrocyclic ring openings of 2-furylcarbene and related carbenes,[8] the [1,3], [3,3], and [3,5] sigmatropic rearrangements of esters,[9] and the torquoselectivity of α- and β-substituted vinyl phenyl isocianates,[10] are some relevant examples of chemical reactivity issues concerning these reactions that have been addressed recently.

Although the orbital concept remains to be central in the understanding and rationalization of pericyclic chemical reaction mechanisms within the basis provided by the Woodward–Hoffmann framework,[12] fundamental questions regarding the intrinsic nature of the bonding formation/bonding breaking at the transition state remains to be further investigated.[1–11] In the framework of consistent ways of characterization of chemical bonding beyond the scope of orbital-dependent treatments, topological analysis (i.e., gradient field analysis) of well-defined local functions provides a powerful approximation to a rigorous quantitative and qualitative analysis. The atoms-in-molecules (AIM) theory of Bader[13] and the Savin, Silvi *et al.*[14] analysis of the electron localization function (ELF) of Becke and Edgecombe,[15] provide us with a useful and convenient partition of the molecular space into basins of attractors that can be related to the intuitive concepts of chemical bonding. In the AIM theory such open subsystems (i.e., basins) are associated with ''atoms,'' while in the ELF scheme they are associated with ''pair regions.''[14] Because we are more interested here in exploring the reaction mechanism topologies at pericyclic and pseudopericyclic transition structures, we have resorted to the ELF picture of bonding. Previous work on benchmark pericyclic reactions corresponding to the $[1_s,3_a]$-hydrogen, $[1_a,3_s]$-methyl, and $[1_a,3_s]$-fluorine[16] sigmatropic shifts in the allyl system have emphasized the usefulness of the analysis of properties of the electron density, integrated over the ELF basins, to obtain a clear picture of electronic rearrangement which is complementary to the traditionally used Woodward–Hoffmann analysis. We present here the first results from an ongoing systematic study concerning the characterization of bonding at pericyclic and pseudopericyclic transition states using the ELF analysis. Our goal is to explore it as a possible descriptor of the electron rearrangement involved along these fundamental types of chemical reactions.

Comprehensive reviews concerning the details of this technique of topological analysis have been published elsewhere.[14,17] A wide range of useful applications of these tools in the examination of chemical bond both at stationary and reacting systems can be found over many different fields of chemistry.[18]

Briefly, the scaled function ELF was defined by Becke and Edgecombe in the framework of a Taylor expansion characterization of the pair density function $P(r,s) = \frac{1}{2}s^2T(r) + \cdots$.[14,15,17] The ELF will acquire values close to 1 within a pair region, and it will be close to 0 in the border

[a)]Electronic mail: echamorro@unab.cl

between two such pair regions. Being the homogeneous electron gas taken as a reference for normalization, the ELF will have the value $\frac{1}{2}$ everywhere in the latest case. The local function ELF($\mathbf{r}$) can therefore be written and interpreted in terms of the excess of local kinetic energy density due to the Pauli repulsion, $T(\rho(r))$, and the Thomas–Fermi kinetic energy density, $T_h(\rho(r))$,[14,17]

$$\mathrm{ELF}(\mathbf{r})=\left[1+\left[\frac{T(\mathbf{r})}{T_h(\mathbf{r})}\right]^2\right]^{-1}. \tag{1}$$

For an arbitrary single determinantal (i.e., a single Slater determinant) wave function, built from Hartree–Fock (HF) or Kohn–Sham (KS) orbitals, $\varphi_i(r)$, it can be straightforward written that

$$T(\mathbf{r})=\frac{1}{2}\sum_i |\nabla\varphi_i(\mathbf{r})|^2-\frac{1}{8}\frac{|\nabla\rho(\mathbf{r})|^2}{\rho(\mathbf{r})}, \tag{2}$$

$$T_h(\mathbf{r})=2.871\rho(\mathbf{r})^{5/3}, \tag{3}$$

$$\rho(\mathbf{r})=\sum_i |\varphi_i(\mathbf{r})|^2, \tag{4}$$

where atomic units are implicit in the equations. The integration of density $\rho(\mathbf{r})$ over the basins of attractors associated with the gradient field of the ELF, yields to properties that can be consistently *interpreted* in connection with relevant chemical bonding characteristics. In this context, the intuitive concepts of localization and delocalization of the electron density[19] are recovered through a standard topological population analysis which is consistent with the Heisenberg uncertainly principle.[17(b),17(c)] The average population of a basin, $\tilde{N}_i$, obtained from the integral of the one electron density over the volume of the basin,

$$\tilde{N}_i=\int_{\Omega_i}\rho(\mathbf{r})dr, \tag{5}$$

and their population variance, $\sigma^2(\tilde{N}_i)$ (i.e., the quantum uncertainty of the basin population), can be calculated in terms of the diagonal elements of the first $\rho(\mathbf{r})$ and second order $\pi(\mathbf{r}_1,\mathbf{r}_2)$ density matrices,

$$\sigma^2(\tilde{N}_i)=\int_{\Omega_i}d\mathbf{r}_1\int_{\Omega_i}d\mathbf{r}_2\pi(\mathbf{r}_1,\mathbf{r}_2)+\tilde{N}_i-[\tilde{N}_i]^2. \tag{6}$$

It has been shown that the variance of a given basin population can be written explicitly in terms of a sum of contributions arising from the other basins,

$$\begin{aligned}\sigma^2(\tilde{N}_i)&=\sum_{j\neq i}\tilde{N}_i\tilde{N}_j-B_{ij},\\ B_{ij}&=\int_{\Omega_i}d\mathbf{r}_1\int_{\Omega_j}d\mathbf{r}_2\rho(\mathbf{r}_1)\rho(\mathbf{r}_2)\\ &\quad+\int_{\Omega_i}d\mathbf{r}_1\int_{\Omega_j}d\mathbf{r}_2\rho_{\mathrm{XC}}(\mathbf{r}_1,\mathbf{r}_2),\end{aligned} \tag{7}$$

where $\rho_{\mathrm{XC}}(\mathbf{r}_1,\mathbf{r}_2)$ stands for the exchange-correlation density.[17,20] Henceforth, the covariance (i.e., interbasin) analysis seems to be a useful tool for a detailed examination of the electronic delocalization in the molecular framework.[20] Indeed, the Bader relative fluctuation index $\lambda(\tilde{N}_i)$, has been also shown an efficient tool to study delocalization,

$$\lambda(\tilde{N}_i)=\frac{\sigma^2(\tilde{N}_i)}{\tilde{N}_i}. \tag{8}$$

With the aim to get further insights about fundamental differences between pericyclic and pseudopericyclic topologies, in this work we have examined the nature of bonding of selected thermal chelotropic decarbonylations transition states from the topological analysis of the electron localization function (ELF). We have chosen those systems of thermal decarbonylations which have been carefully reviewed and examined by Birney *et al.* in light of the orbital symmetry rules.[11] It will be clear that the lack of cyclic ''orbital''

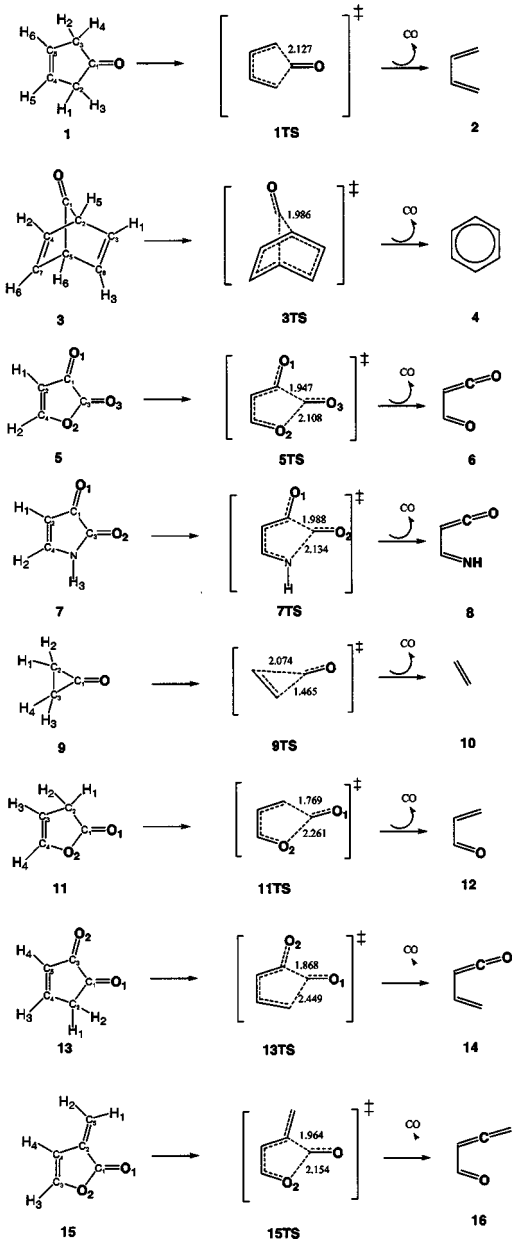

FIG. 1. Schematic view and numbering of the eight thermal chelotropic decarbonylations studied in this work.

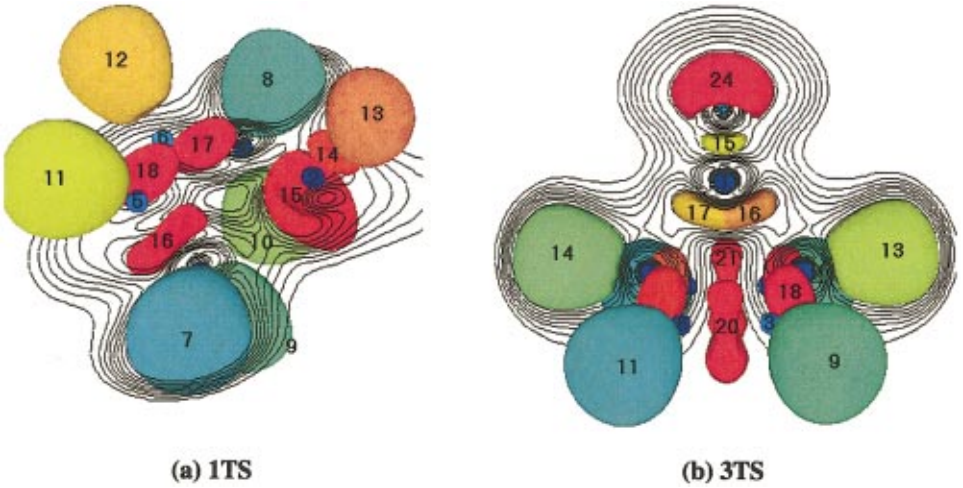

FIG. 2. (Color) Localization domains of the electron localization function (ELF) at the 1TS and 3TS transition states. The ELF=0.82 isosurfaces were calculated from the optimized wave functions at the MP2(FC)/6-31G(d) level of theory.

overlap in pseudopericyclic reactions should be apparent from the noncyclic pattern of electron fluctuations between the populations in the ELF basins.

II. COMPUTATIONAL DETAILS

The *ab initio* MP2(FC)/6-31G* optimized transition states corresponding to the eight thermal chelotropic decarbonylations schematized in Fig. 1 have been obtained from the corresponding supporting information of Ref. 11. The wave functions have been built in using the GAUSSIAN 98 package of programs.[21] The topological analysis of the ELF and its associated population analysis have been performed using the TOPMOD suite of programs.[22,23] Graphical analysis was done using the Vis5d (Ref. 24) visualization tools.

III. RESULTS AND DISCUSSION

It will be remarked that the present analysis yields a picture for pericyclic and pseudopericyclic reactions which does not use the orbital-based picture of bonding. However, it must be remarked that there is clear relation between the ELF and the nodal orbital structure of molecules and solids.[25] Being the ELF a robust technique of analysis almost independent of method of calculation yielding a suitable wave function, we do not resort to any type of orbital hybridization *concepts* to explore the bonding nature at these transition states.[11] The topologies of the electron localization domains, represented by the ELF=0.82 isosurfaces, for the eight pericyclic transition structures are depicted in Figs. 2, 4, and 6. The corresponding bifurcation diagrams are depicted in Figs. 3, 5, and 7. The results from the ELF topological population analysis, including the basin populations $\widetilde{N}_i$, associated variances $\sigma^2(\widetilde{N}_i)$, relative fluctuation $\lambda(\widetilde{N}_i)$, and main contributions from other basins $i(\%)$ to $\sigma^2(\widetilde{N}_i)$ for each TS, are reported in Tables I–VIII. Although core basin populations and related properties have not a relevant role for the description of the observed reactivity along the sigmatropic rearrangements, this information have been retained only for completeness of the present analysis.

A. The nature of the CO leaving group

It has been emphasized previously that for the eight transition states, the departing CO can be drawn as carbon monoxide with a lone pair on the carbon atom. Of course, alternative schemes of hybridization can be also considered, specifically for the case of transitions states 9TS and 11TS. From Tables I–VIII, a consistent picture of bonding can be drawn from the ELF analysis: two core basins which are associated with the C and O atoms, one (or two) disynaptic valence basins associated with the C–O bond region, one (or two) monosynaptic valence basins corresponding to the lone

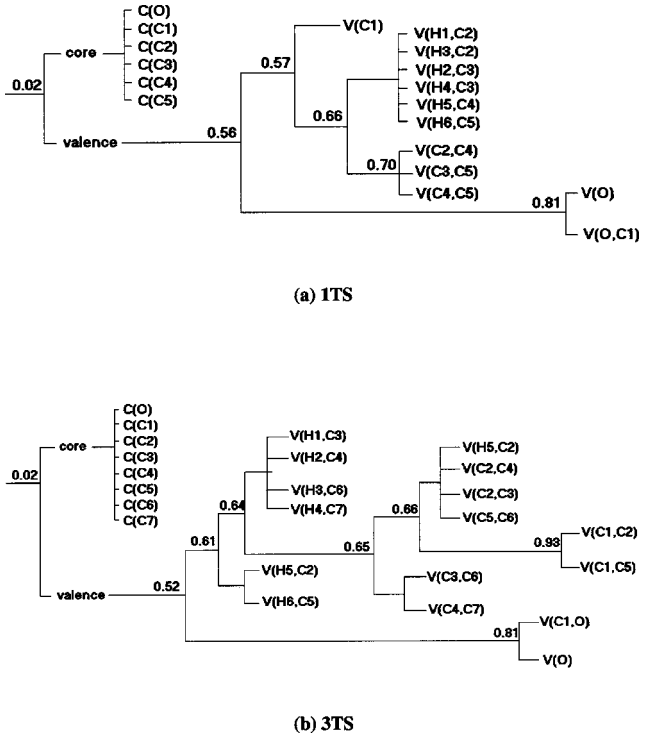

FIG. 3. Bifurcation diagrams corresponding to the electron localization function (ELF) analysis at the 1TS and 3TS transition states from the optimized wave functions at the MP2/6-31G(d) level of theory.

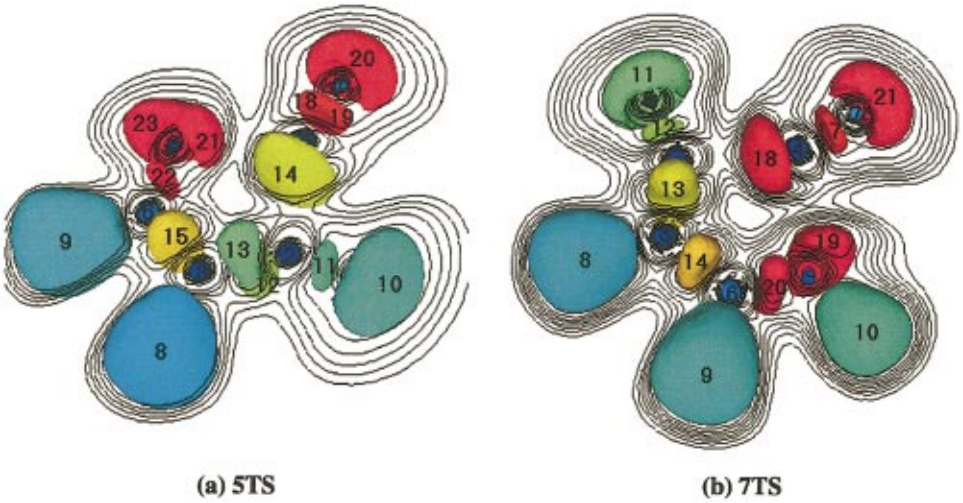

FIG. 4. (Color) Localization domains of the electron localization function (ELF) at the 5TS and 7TS transition states. The ELF=0.80 isosurfaces were calculated from the optimized wave functions at the MP2(FC)/6-31G(d) level of theory.

pair region of oxygen, and one (or two) monosynaptic or disynaptic basins associated with the lone pair region of the carbon atom at the departing CO. Very small charge separations could be established from a naive partition based on the basin populations independently. However, it must be clear that pronounced electron fluctuations are present between both the CO and the remaining fragment at the center of reaction.

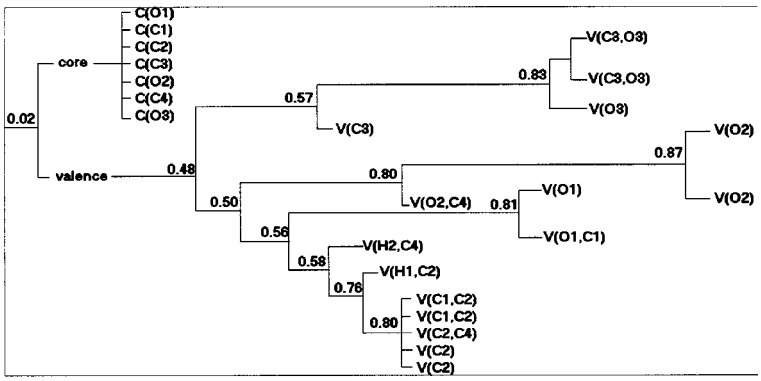

(a) 5TS

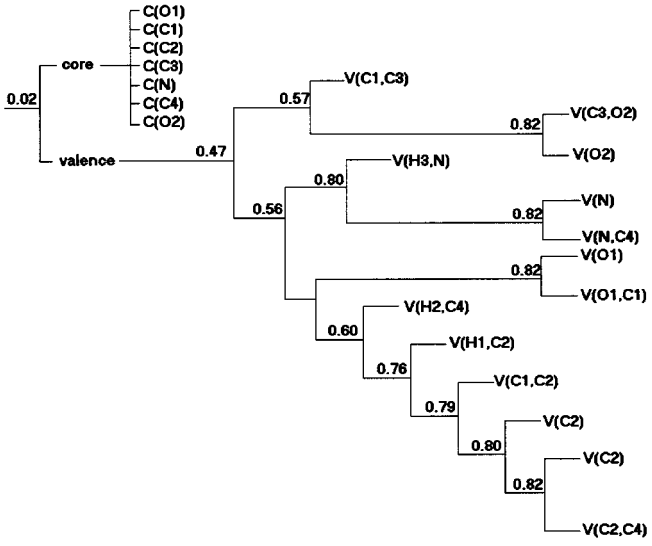

(b) 7TS

FIG. 5. Bifurcation diagrams corresponding to the electron localization function (ELF) analysis at the 5TS and 7TS, transition states from the optimized wave functions at the MP2/6-31G(d) level of theory.

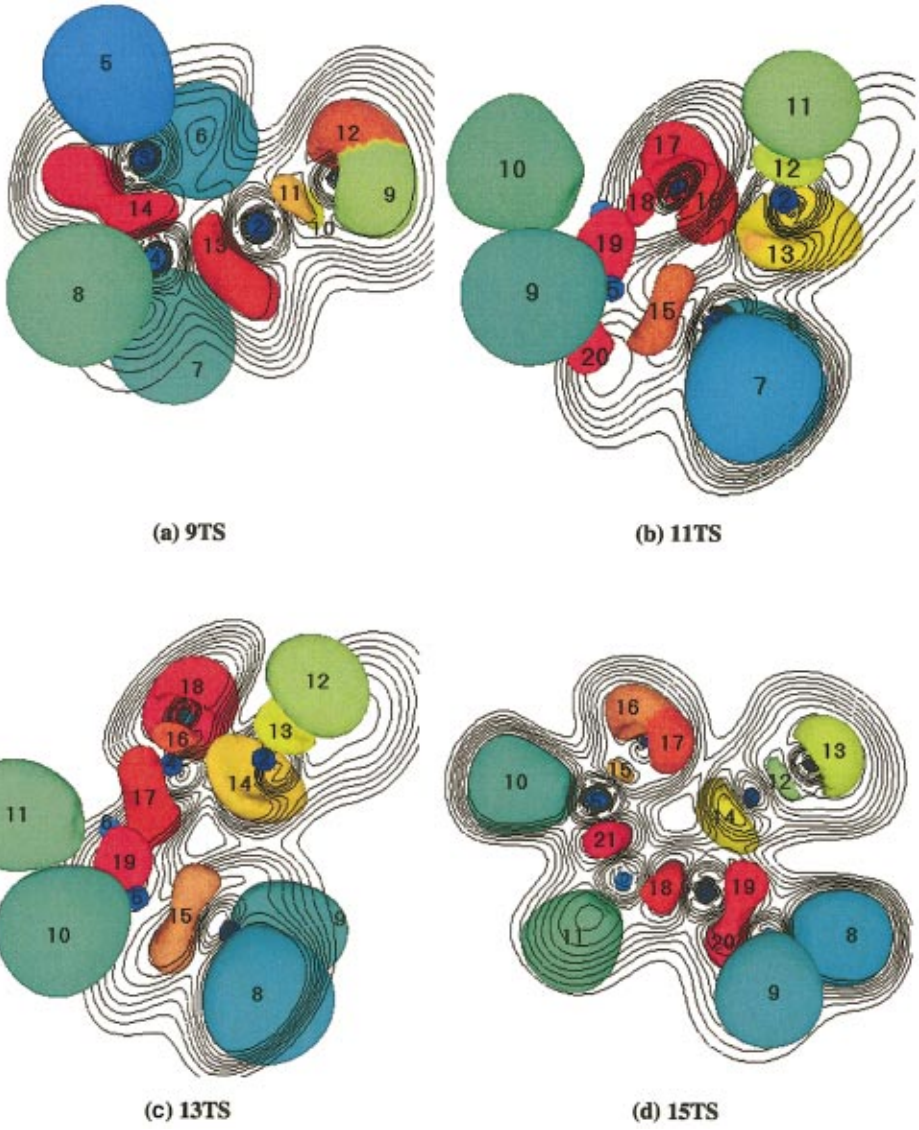

FIG. 6. (Color) Localization domains of the electron localization function (ELF) at the 9TS, 11TS, 13TS, and 15TS transition states. The ELF=0.80 isosurfaces were calculated from the optimized wave functions at the MP2(FC)/6-31G(d) level of theory.

B. Pericyclic reactions: Cyclic orbital overlap: 1TS and 3TS

It is known that the decarbonylation of 3-cyclopentenona (1) via the transition state 1TS has been described like a typical concerted pericyclic reaction where the CO departure from the butadiene plane involves an orbital symmetry allowed disrotatory pathway with C_s symmetry.[11] From Table I and Fig. 2(a), the ELF topology of 1TS reveals a monosynaptic valence basin V(C1) localizing $2.41e-$. This population at the extremum of the leaving C1 carbon atom, has associated a high value of variance, $\sigma^2=1.07$, while a delocalization index $\lambda=0.45$ is consistent with an appreciable fluctuation. The analysis of main contributions of other basin populations to the variance, point out that main fluctuations arise from the monosynaptic V(O) (19.3%) and the disynaptic V(O,C1) (23.0%) valence basin populations associated with the oxygen lone pairs region ($4.62e-$) and the C1–O bonding ($2.91e-$), respectively. It is clear that a picture of bonding at the present level of theory remarks a small localization of charge corresponding to $0.11e$ toward the departing CO at the transition state. In the framework of topological analysis, the effects of the level of calculation [i.e., the exchange-correlation terms involved in the evaluation of second order matrix in Eq. (6)], on the topological population analysis has been already explored. See, for instance, Ref. 20. However, it must be also clear that a noticeable fluctuation contribution corresponding to 11.0% is arising from the equivalent V(C2,C4) and V(C3,C5) basin populations, which localize $3.08e-$ each. Furthermore, the V(C4,C5) basin population ($2.68e-$) is related to (i.e., delocalized over) the V(C2,C4) and V(C3,C5) basin populations up to 21.9%. The co-variance analysis based on Eq. (6) reveals that the electronic changes in the butadiene fragment are strongly interrelated with the departure of the CO through a cyclic symmetric pattern of electron fluctuations involving the ELF basins. Looking at the leaving CO group, main contributions to the V(C1) basin are coming from the V(O) population (19.0%) and from the V(C1,O) basin population (23.0%). Furthermore, we can note from the structure of the bifurcation diagram corresponding to 1TS in Fig. 3(a), that a unique reducible domain yielding the V(C1) basin separates early at ELF=057. This is consistent with the strong correlation pat-

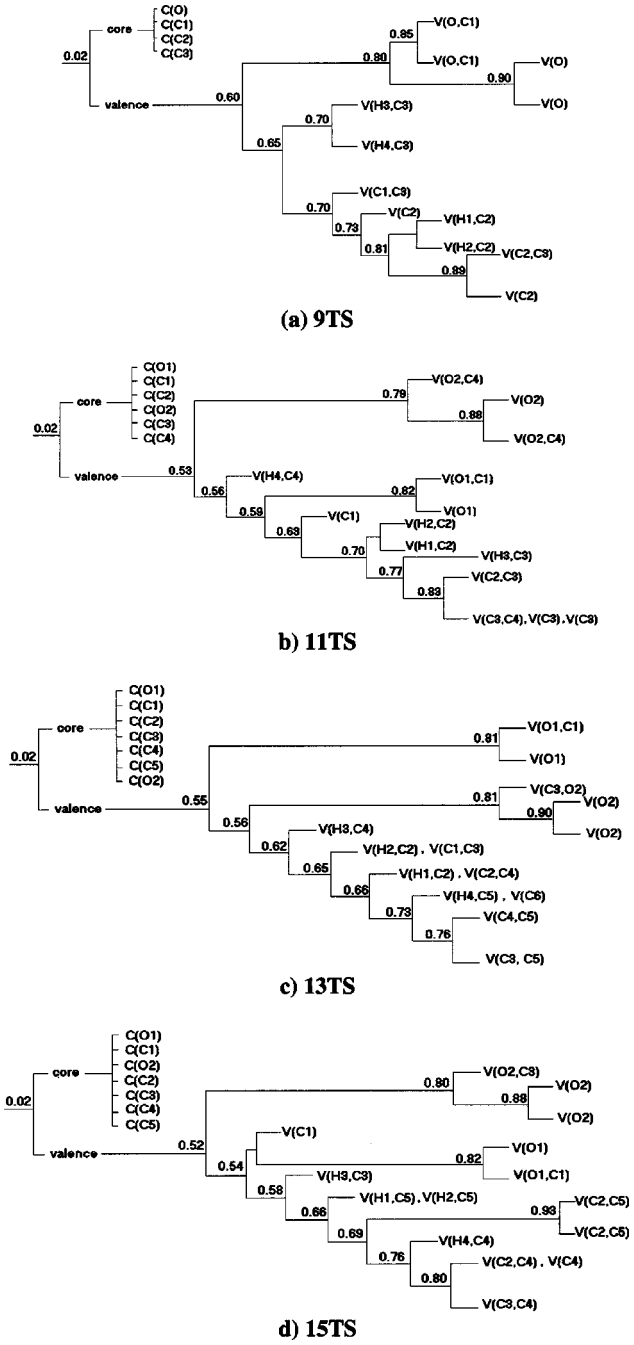

FIG. 7. Bifurcation diagrams corresponding to the electron localization function (ELF) analysis at the 9TS, 11TS, 13TS, and 15TS, transition states from the optimized wave functions at the MP2/6-31G(d) level of theory.

tern observed at the leaving CO and butadiene fragments alone. The reducible domain corresponding to all the C–H, and C–C bonds at the butadiene fragment, does bifurcate at ELF=0.66, and ELF=0.70, respectively. The appreciable correlation at the CO fragment is also clear from the V(O) and V(O,C1) basin domain separations at higher ELF value.

The decarbonylation of bicycle[2.2.1]hepta-2,5-dien-7-one (3) through the C_{2v} transition state 3TS follows also an allowed disrotatory (linear-suprafacial) pathway.[11] From Table II and Fig. 2(b), we can note again a cyclic and symmetric pattern of delocalization at the 3TS which can be drawn directly from the co-variance analysis. The electron fluctuation (i.e., delocalization) appears to be more extended in 3TS than in 1TS. Thus, we have that two valence disynaptic basins V(C1,C2) and V(C1,C5), both with 1.52e, can be explicitly localized in the ELF gradient field of 3TS. Associated variances are very appreciable ($\sigma^2=0.93$), and the corresponding fluctuation indexes are the highest ones in the system ($\lambda=0.61$). Like in the case of 1TS, strong correlations can be observed both in the CO group as well as in the remaining fragment, although a formal separation between them is not possible. The pattern of fluctuation indicates that complementarily to the CO self-delocalization, main contributions to these populations arise from the symmetric V(C,C) and V(C,H) closets neighbors basins. For instance, for the V(C1,C2) basin population we found contributions from V(H5,C2), V(C1,O), V(C1,C5), V(C2,C3), V(C2,C4), V(O) population basins corresponding to 9.1%, 13.3%, 21.4% 10.9%, 10.9%, and 10.7%, respectively. Note that similar results are obtained for the V(C1,C5) basin population. Thus, it is clear that a cyclic pattern of delocalization is also present between the V(C,C) and V(C,H) basin populations. Contributions arising from the V(C,H) population basins toward the adjacent basins are approximately 15%, and the V(C,C) population fluctuates in the range of 10%–23%. This picture of pericyclic bonding is being reinforced by the bifurcation diagram depicted in Fig. 3(b). We note for instance that the reducible domain which separate at ELF=0.61–0.66 accounts for all the valence basins corresponding to the C–H and C–C bonding interactions. Indeed, correspondingly with the highest values of delocalization parameter, $\lambda=0.65$, the V(C1,C2) and V(C1,C5) are being reduced only at higher ELF values.

In summary, the ELF results obtained both for the 1TS and 3TS pericyclic transition states, agrees with an intuitive picture of bonding which yields to a cyclic delocalization pattern along the electronic rearrangement at the departure of the CO. The electron population and related variance analysis based on the ELF basin populations seem to be a suitable complement to the traditionally used orbital symmetry rules based analysis.

C. Pseudopericyclic reactions: Two orbital disconnections: 5TS and 7TS

The decarbonylation of furandione (5) through the orbital symmetry allowed transition state 5TS has been described implying a pseudopericyclic topology, with two orbital disconnections when the CO departs in the plane of the molecule.[11] From Table III and Fig. 3(a), we can observe a valence monosynaptic V(C1) basin localizing 2.29e ($\sigma^2=0.97$, $\lambda=0.42$) at the extremum of the departing CO. In this case however, there is not, in effect, any cyclic interrelation with the remaining fragment. We note immediately that main contribution to this high variance corresponds to 19.9%, 12.9%, and 12.8%, which are arising from the V(O3) basin population, and the two V(C3,O3) basins in the CO fragment, respectively. On the other hand, contributions from the V(O1) basin, the V(O1,C1) basin, the two V(C1,C2) basins, and the lone pair population which is associated with the V(O2) basin, are only 6.1%, 8.1%, 6.2% each, and 7.5%, respectively. There is a very small (i.e., 0.02e) or null sepa-

TABLE I. Basin populations $\bar{N}_i$, standard deviation $\sigma^2(\bar{N}_i)$, relative fluctuation $\lambda(\bar{N}_i)$, and main contributions of other basins $i(\%)$ to $\sigma^2(\bar{N}_i)$ for the 1TS transition state from the density obtained at the MP2(FC)/6-31G* level of theory.

Basin		$\bar{N}_i$	$\sigma^2(\bar{N}_i)$	$\lambda(\bar{N}_i)$	Contribution analysis (%)
1	C(O)	2.11	0.35	0.17	13(62.6) 14(31.8)
2	C(C1)	2.06	0.23	0.11	13(13.2) 14(35.4) 15(43.1)
3	C(C2)	2.07	0.25	0.12	7(28.1) 9(28.8) 16(34.4)
4	C(C3)	2.07	0.25	0.12	8(28.1) 10(28.8) 17(34.2)
5	C(C4)	2.09	0.26	0.12	11(28.1) 16(32.4) 18(29.7)
6	C(C5)	2.09	0.26	0.12	12(28.1) 17(32.4) 18(29.7)
7	V(H1,C2)	2.13	0.63	0.3	3(11.0) 9(30.2) 15(4.9) 16(39.9)
8	V(H2,C3)	2.13	0.63	0.3	4(11.0) 10(30.2) 15(4.9) 17(39.9)
9	V(H3,C2)	2.12	0.67	0.31	3(10.8) 7(28.7) 15(9.9) 16(36.0)
10	V(H4,C3)	2.12	0.67	0.31	4(10.8) 7(28.7) 15(9.9) 17(36.0)
11	V(H5,C4)	2.12	0.63	0.3	5(11.3) 16(37.0) 18(32.5)
12	V(H6,C5)	2.12	0.63	0.3	6(11.4) 17(37.0) 18(32.5)
13	V(O)	4.62	1.42	0.31	1(15.3) 14(63.6) 15(14.5)
14	V(O,C1)	2.91	1.4	0.48	1(7.9) 2(5.8) 13(64.9) 15(17.7)
15	V(C1)	2.41	1.07	0.45	2(9.1) 9(6.2) 10(6.2) 13(19.3) 14(23.0) 16(11.1) 17(11.1)
16	V(C2,C4)	3.08	1.42	0.46	3(6.0) 5(5.8) 7(17.7) 9(16.8) 11(16.5) 15(8.3) 18(19.4)
17	V(C3,C5)	3.08	1.42	0.46	4(6.0) 6(5.8) 8(17.7) 10(16.8) 12(16.5) 15(8.3) 18(19.4)
18	V(C4,C5)	2.68	1.26	0.47	5(6.0) 6(6.0) 11(16.3) 12(16.3) 16(21.9) 17(21.9)

ration of charge at the 5TS stationary point by considering the CO and the remaining fragment separately. This pattern of fluctuation can be straightforward related with the corresponding bifurcation diagram depicted in Fig. 5(a). The bifurcation at a low value of ELF=0.48 yields directly to the separation into the V(C3)UV(C3,O3)UV(C3,O3)UV(O3) domain, and the remaining basins associated with the O1–C1–C2–C4–O2 chain. The variance and localization values which are associated with these populations agree explicitly with ELF values in the bifurcation diagram. Highest values correspond naturally to the separation of domains associated with the interaction regions of C–O bonds and the oxygen lone pair region. Furthermore, the ELF analysis reveals a clear an intuitive image about the intrinsic electronic changes along the reaction pathway. For instance, we can note that the highly delocalized two valence monosynaptic V(C2) basins ($0.43e$, $\sigma^2=0.36$, $\lambda=0.84$) which are arising only like an intimate part of the rearranging density at the C1–C2 and C2–C4 bond order change at the TS.

A comparison between the 1TS and 5TS is useful in

TABLE II. Basin populations $\bar{N}_i$, standard deviation $\sigma^2(\bar{N}_i)$, relative fluctuation $\lambda(\bar{N}_i)$, and main contributions of other basins $i(\%)$ to $\sigma^2(\bar{N}_i)$ for the 3TS from the density obtained at the MP2(FC)/6-31G* level of theory.

Basin		$\bar{N}_i$	$\sigma^2(\bar{N}_i)$	$\lambda(\bar{N}_i)$	Contribution analysis (%)
1	C(C1)	2.07	0.23	0.11	15(34.5) 16(21.7) 17(21.7) 24(13.2)
2	C(C2)	2.07	0.25	0.12	13(29.5) 16(7.3) 18(26.3) 19(26.3)
3	C(C3)	2.08	0.26	0.12	9(28.4) 18(25.8) 20(36.0)
4	C(C4)	2.08	0.26	0.12	10(28.4) 19(25.8) 4(36.0)
5	C(C5)	2.07	0.25	0.12	14(29.5) 17(7.3) 22(26.3) 23(26.3)
6	C(C6)	2.08	0.26	0.12	11(28.4) 20(36.0) 22(25.8)
7	C(C7)	2.08	0.26	0.12	12(28.4) 23(25.8)
8	C(O)	2.12	0.35	0.16	15(28.7) 24(65.8)
9	V(H1,C3)	2.14	0.63	0.3	3(11.5) 18(26.5) 20(43.6)
10	V(H2,C4)	2.14	0.63	0.3	4(11.5) 19(26.5) 20(43.4) 21(43.6)
11	V(H3,C6)	2.14	0.63	0.3	6(11.5) 22(26.5)
12	V(H4,C7)	2.14	0.63	0.3	7(11.5) 21(43.6) 23(26.5)
13	V(H5,C2)	2.15	0.64	0.3	2(11.6) 16(13.3) 18(27.2) 19(27.2)
14	V(H6,C5)	2.15	0.64	0.3	5(11.6) 17(13.3) 22(27.2) 23(27.2)
15	V(C1,O)	2.82	1.38	0.49	1(5.8) 8(7.2) 16(8.9) 17(8.9) 24(65.9)
16	V(C1,C2)	1.52	0.93	0.61	1(5.4) 13(9.1) 15(13.3) 17(21.4) 18(10.9) 19(10.9) 24(10.7)
17	V(C1,C5)	1.52	0.93	0.61	1(5.4) 14(9.1) 15(13.3) 16(21.4) 22(10.9) 23(10.9) 24(10.7)
18	V(C2,C3)	2.29	1.12	0.49	2(5.9) 3(5.9) 9(15.0) 13(15.5) 16(9.0) 19(13.9) 20(22.9)
19	V(C2,C4)	2.29	1.12	0.49	2(5.9) 4(5.9) 10(15.0) 13(15.5) 18(13.9) 21(22.9)
20	V(C3,C6)	3.34	1.45	0.43	3(6.4) 7(6.4) 10(19.0) 11(19.0) 18(17.7) 22(17.7)
21	V(C4,C7)	3.34	1.45	0.43	4(6.4) 7(6.4) 10(19.0) 12(19.0) 19(17.7) 23(17.7)
22	V(C5,C6)	2.29	1.12	0.49	5(5.9) 6(5.9) 11(15.0) 14(15.5) 17(9.0) 20(22.9) 23(13.9)
23	V(C5,C7)	2.29	1.12	0.49	5(5.9) 7(5.9) 12(15.0) 14(15.5) 17(9.0) 21(22.9) 22(13.9)
24	V(O)	4.76	1.43	0.3	7(15.9) 15(63.7) 16(6.9) 17(6.9)

TABLE III. Basin populations $\bar{N}_i$, standard deviation $\sigma^2(\bar{N}_i)$, relative fluctuation $\lambda(\bar{N}_i)$, and main contributions of other basins $i(\%)$ to $\sigma^2(\bar{N}_i)$ for the 5TS from the density obtained at the MP2(FC)/6-31G* level of theory.

	Basin	$\bar{N}_i$	$\sigma^2(\bar{N}_i)$	$\lambda(\bar{N}_i)$	Contribution analysis (%)
1	C(O1)	2.13	0.35	0.16	10(71.5) 11(23.5)
2	C(C1)	2.08	0.24	0.11	10(13.4) 11(34.4) 12(19.6) 13(19.4)
3	C(C2)	2.09	0.26	0.13	7(27.5) 12(14.1) 13(14.0) 15(26.3) 16(5.4) 17(5.4)
4	C(C3)	2.07	0.23	0.11	14(41.4) 18(19.0) 19(19.2) 20(14.0)
5	C(O2)	2.14	0.35	0.16	21(33.7) 22(19.6) 23(40.2)
6	C(C4)	2.08	0.25	0.12	9(30.2) 15(27.9) 22(25.2) 23(5.9)
7	C(O3)	2.1	0.34	0.16	18(17.3) 19(17.5) 20(59.8)
8	V(H1,C2)	2.06	0.66	0.32	3(10.9) 12(14.6) 13(14.5) 15(23.4) 16(11.7) 17(11.7)
9	V(H2,C4)	2.12	0.57	0.27	6(13.1) 15(29.5) 21(7.1) 22(23.8) 23(12.3)
10	V(O1)	5.19	1.42	0.27	1(17.4) 11(61.8)
11	V(O1,C1)	2.56	1.36	0.53	1(6.0) 2(6.1) 10(64.6) 12(6.7) 13(6.6) 14(5.7)
12	V(C1,C2)	1.41	0.86	0.61	2(5.5) 8(11.3) 10(6.7) 11(10.6) 13(26.1) 14(7.1) 15(11.2) 17(10.0)
13	V(C1,C2)	1.39	0.85	0.61	2(5.4) 8(11.3) 10(6.6) 11(10.5) 12(26.3) 14(7.1) 15(11.2) 16(10.1)
14	V(C3)	2.29	0.97	0.42	4(9.9) 10(6.1) 11(8.1) 12(6.3) 13(6.2) 18(12.8) 19(12.9) 20(19.7) 21(7.5)
15	V(C2,C4)	2.31	1.09	0.47	3(6.3) 6(6.3) 8(14.2) 9(15.3) 12(8.8) 13(8.7) 16(8.0) 17(8.0) 22(11.9)
16	V(C2)	0.43	0.36	0.84	8(21.2) 12(6.2) 13(23.5) 15(24.0) 17(5.8)
17	V(C2)	0.43	0.36	0.84	8(21.2) 12(23.6) 13(6.2) 15(24.0) 16(5.8)
18	V(C3,O3)	1.57	0.98	0.62	7(6.1) 14(12.7) 19(26.0) 20(48.2)
19	V(C3,O3)	1.6	0.98	0.62	7(6.1) 14(12.7) 18(25.7) 20(48.4)
20	V(O3)	4.39	1.41	0.32	7(14.6) 14(13.5) 18(33.3) 19(33.8)
21	V(O2)	2.47	1.2	0.49	5(9.7) 14(6.1) 22(27.6) 23(42.8)
22	V(O2,C4)	2.12	1.19	0.56	5(5.7) 6(5.2) 9(11.3) 15(10.9) 21(27.8) 23(34.7)
23	V(O2)	2.98	1.26	0.42	5(11.0) 9(5.5) 21(40.7) 22(32.8)

order to establish the main differences between both pericyclic and pseudopericyclic topologies. At first, we can see that the concept of ''disconnection'' involved in an orbital framework, here can be replaced by the examination of direct electron fluctuation at the interaction centers. In effect is clear that there are no electrons being exchanged between the basins associated with the O2–C3 breaking at 5TS. The O2 lone pair regions is not delocalized significantly (approximately 7.5%) over the 2.29e which are centered at the carbon atom of the leaving CO.

Decarbonylation of 2,3-pyrroledione (7) via the transition state 7TS is also a concerted and asynchronous pseudopericyclic reaction.[11] The process has been drawn like the interaction of a CO lone pair with the imidoylketene. Table IV and Fig. 4(b) reveals a valence disynaptic V(C1,C3) basin localizing a population of 2.32e ($\sigma^2=0.98$, $\lambda=0.42$) which naturally emerges in the corresponding gradient field of the ELF. Main contributions from the imidoylketene are coming from the V(C1,C2) basin population (12.0%), and the fluctuation from the nitrogen lone pair region is lower

TABLE IV. Basin population $\bar{N}_i$, standard deviation $\sigma^2(\bar{N}_i)$, relative fluctuation $\lambda(\bar{N}_i)$, and main contributions of other basins $i(\%)$ to $\sigma^2(\bar{N}_i)$ for the 7TS from the density obtained at the MP2(FC)/6-31G* level of theory.

	Basin	$\bar{N}_i$	$\sigma^2(\bar{N}_i)$	$\lambda(\bar{N}_i)$	Contribution analysis (%)
1	C(O1)	2.06	0.34	0.17	11(73.6) 12(22)
2	C(C1)	2.08	0.24	0.12	11(13.3) 12(33.8) 13(39.8)
3	C(C2)	2.09	0.26	0.12	8(27.3) 13(28.3) 14(25.4) 15(6.1) 16(5.4)
4	C(C3)	2.06	0.23	0.11	17(35.4) 18(43.2) 21(14.6)
5	C(N)	2.09	0.3	0.14	10(24.4) 19(40.5) 20(28.0)
6	C(C4)	2.09	0.25	0.12	9(28.8) 14(27.0) 19(5.4) 20(30.6)
7	C(O2)	2.07	0.34	0.16	17(32.1) 21(62.7)
8	V(H1,C2)	2.05	0.66	0.32	3(10.8) 13(30.2) 14(22.6) 15(11.8) 16(11.3)
9	V(H2,C4)	2.12	0.59	0.28	6(12.3) 14(27.8) 19(10.1) 20(32.6)
10	V(H3,N)	1.99	0.75	0.38	5(9.6) 19(46.0) 20(32.4)
11	V(O1)	5.26	1.43	0.27	1(17.6) 12(61.4) 13(8.3)
12	V(O1,C1)	2.56	1.35	0.53	1(5.6) 2(6.0) 11(64.9) 13(13.7) 18(5.4)
13	V(C1,C2)	2.89	1.29	0.45	2(7.5) 3(5.7) 8(15.5) 11(9.2) 12(14.4) 14(14.4) 15(9.1) 16(8.7) 18(9.2)
14	V(C2,C4)	2.25	1.08	0.48	3(6.1) 6(6.3) 8(13.8) 9(15.2) 13(17.1) 15(7.7) 16(7.2) 20(15.7)
15	V(C2)	0.44	0.37	0.84	8(21.0) 13(31.7) 14(22.4) 16(5.3)
16	V(C2)	0.41	0.35	0.85	8(21.2) 13(31.5) 14(22.0) 15(5.6)
17	V(C3,O2)	3.05	1.42	0.47	4(5.7) 7(7.7) 18(16.8) 21(66.3)
18	V(C1,C3)	2.32	0.98	0.42	4(10.0) 11(5.7) 12(7.4) 13(12.0) 17(24.4) 19(9.8) 21(20.6)
19	V(N)	2.85	1.27	0.44	5(9.5) 10(27.4) 18(7.6) 20(37.5)
20	V(N,C4)	2.72	1.32	0.49	5(6.3) 6(5.8) 9(14.6) 10(18.4) 14(12.9) 19(35.9)
21	V(O2)	4.53	1.44	0.32	7(14.5) 17(65.7) 18(14.1)

TABLE V. Basin population $\tilde{N}_i$, standard deviation $\sigma^2(\tilde{N}_i)$, relative fluctuation $\lambda(\tilde{N}_i)$, and main contributions of other basins $i(\%)$ to $\sigma^2(\tilde{N}_i)$ for the 9TS from the density obtained at the MP2(FC)/6-31G* level of theory.

Basin		$\tilde{N}_i$	$\sigma^2(\tilde{N}_i)$	$\lambda(\tilde{N}_i)$	Contribution analysis (%)
1	C(O)	2.17	0.35	0.16	9(33.2) 10(13.2) 11(13.2) 12(34.9)
2	C(C1)	2.06	0.23	0.11	9(6.2) 10(17.2) 11(17.2) 12(6.6) 13(41.4)
3	C(C2)	2.09	0.25	0.12	5(26.8) 6(26.8) 14(19.5) 15(14.0)
4	C(C3)	2.09	0.25	0.12	7(27.0) 8(27.7) 13(17.3) 14(22.6)
5	V(H1,C2)	2.09	0.67	0.32	3(10.1) 6(24.9) 13(7.8) 14(17.5) 15(21.4) 16(8.6)
6	V(H2,C2)	2.09	0.67	0.32	3(10.1) 5(24.9) 13(7.8) 14(17.5) 15(21.4) 16(8.6)
7	V(H3,C3)	2.01	0.62	0.31	4(11.0) 8(29.3) 13(25.1) 14(22.3)
8	V(H4,C3)	2.01	0.62	0.31	4(11.0) 7(29.3) 13(25.1) 14(22.3)
9	V(O)	2.41	1.14	0.47	1(10.2) 10(18.9) 1(18.9) 12(39.7) 13(7.2)
10	V(O,C1)	1.33	0.87	0.65	1(5.3) 9(24.8) 11(20.5) 12(26.2) 13(13.3)
11	V(O,C1)	1.33	0.87	0.65	11(5.3) 9(24.8) 10(20.5) 12(26.2) 13(13.3)
12	V(O)	2.57	1.18	0.46	1(10.4) 9(38.5) 10(19.4) 11(19.4) 13(6.8)
13	V(C1,C3)	2.7	1.24	0.46	2(7.8) 7(12.5) 8(12.5) 9(6.6) 10(9.3) 11(9.3) 12(6.4) 14(13.0)
14	V(C2,C3)	1.84	1	0.55	4(5.7) 5(11.6) 6(11.6) 7(13.8) 8(13.8) 13(16.1) 15(15.3)
15	V(C2)	0.91	0.64	0.71	3(5.5) 5(22.3) 6(22.3) 13(9.5) 14(23.8)
16	V(C2)	0.31	0.27	0.89	5(21.0) 6(21.0) 13(18.7) 14(14.8)

than those coming from the from the C1–O1 bonding region. The bifurcation diagram in Fig. 5(b) indicates the strong electron correlation pattern along the C1–C2–C4 line of bonding.

D. Pseudopericyclic reactions: One orbital disconnection: 9TS, 11TS, 13TS, 15TS

Decarbonylation of cyclopropanone (9) through the transition state 9TS implies a very asynchronous planar departure of the CO. It has been suggested that this reaction, although formally orbital symmetry allowed, lacks energy of concert being effectively forbidden.[11] Table V and Fig. 6(a) remarks out that the disynaptic valence V(C1,C3) basin localizing $2.7e$ is associated with the C1–C3 bond breaking at the 9TS. There is a pronounced interaction of electron fluctuation with the V(C2,C3) basin population (13.0%) and through both the V(C3,H3) (12.5%) and V(C3,H4) (12.5%) basin populations. The two highly delocalized monosynaptic basin populations centered in $0.91e$ and $0.31e$, that are associated with the C2 carbon center, can be viewed simply as a result of the rearrangement of the forming C2–C3 double bond. Notice that contributions of 23.8% and 14.8% are coming to these from the V(C2,C3) basin population. The bifurcation diagram in Fig. 7(a) point out more clearly the

TABLE VI. Basin populations $\tilde{N}_i$, standard deviation $\sigma^2(\tilde{N}_i)$, relative fluctuation $\lambda(\tilde{N}_i)$, and main contributions of other basins $i(\%)$ to $\sigma^2(\tilde{N}_i)$ for the 11TS from the density obtained at the MP2(FC)/6-31G* level of theory.

Basin		$\tilde{N}_i$	$\sigma^2(\tilde{N}_i)$	$\lambda(\tilde{N}_i)$	Contribution analysis (%)
1	C(O1)	2.1	0.34	0.16	11(62.3) 12(32.0)
2	C(C1)	2.06	0.23	0.11	11(13.8) 12(37.0) 13(40.7)
3	C(C2)	2.08	0.25	0.12	7(28.5) 8(28.7) 13(6.3) 15(28.1)
4	C(O2)	2.08	0.34	0.16	16(36.8) 17(39.4) 18(17.9)
5	C(C3)	2.09	0.26	0.12	9(27.0) 15(24.2) 19(29.9) 20(9.0)
6	C(C4)	2.08	0.25	0.12	10(29.7) 17(5.2) 18(24.2) 19(29.7)
7	V(H1,C2)	2.07	0.61	0.3	3(11.6) 8(30.1) 13(14.1) 15(27.9)
8	V(H2,C2)	2.05	0.62	0.3	3(11.5) 7(29.7) 13(16.8) 15(25.9)
9	V(H3,C3)	2.1	0.65	0.31	5(10.6) 15(24.1) 19(31.3) 20(16.3)
10	V(H4,C4)	2.14	0.58	0.27	6(12.7) 16(7.4) 17(11.0) 18(23.0) 19(32.3)
11	V(O1)	4.51	1.43	0.32	1(14.9) 12(64.7) 13(13.6)
12	V(O1,C1)	3.04	1.43	0.47	1(7.6) 2(5.9) 11(64.8) 13(16.9)
13	V(C1)	2.34	1.11	0.47	2(8.4) 7(7.8) 8(9.4) 11(17.5) 12(21.8) 15(9.4) 16(5.9)
14	V(C2)	0.09	0.08	0.97	7(9.8) 8(5.5) 12(5.5) 13(55.5) 15(11.8)
15	V(C2,C3)	2.3	1.13	0.49	3(6.2) 5(5.5) 7(15.1) 8(14.2) 9(13.8) 13(9.1) 19(17.7) 20(10.7)
16	V(O2,C4)	2.7	1.24	0.46	4(10.0) 13(5.2) 17(42.0) 18(28.2)
17	V(O2)	2.87	1.22	0.43	4(10.9) 10(5.2) 16(42.8) 18(30.2)
18	V(O2,C4)	2.04	1.17	0.58	4(5.1) 6(5.1) 10(11.3) 16(29.9) 17(31.4) 19(12.2)
19	V(C3,C4)	2.6	1.23	0.47	5(6.3) 6(5.9) 9(16.6) 10(15.1) 15(16.4) 18(11.6) 20(11.3)
20	V(C3)	0.65	0.51	0.78	9(20.8) 13(5.0) 15(23.7) 19(27.2)

TABLE VII. Basin populations $\tilde{N}_i$, standard deviation $\sigma^2(\tilde{N}_i)$, relative fluctuation $\lambda(\tilde{N}_i)$, and main contributions of other basins $i(\%)$ to $\sigma^2(\tilde{N}_i)$ for the 13TS from the density obtained at the MP2(FC)/6-31G* level of theory.

Basin		$\tilde{N}_i$	$\sigma^2(\tilde{N}_i)$	$\lambda(\tilde{N}_i)$	Contribution analysis (%)
1	C(O1)	2.13	0.35	0.16	12(61.6) 13(32.4)
2	C(C1)	2.06	0.23	0.11	12(13.5) 13(36.3) 14(43.2)
3	C(C2)	2.08	0.25	0.12	8(27.9) 9(28.0) 15(37.0)
4	C(C3)	2.08	0.24	0.12	14(5.3) 16(31.5) 17(42.5) 18(6.8) 20(6.3)
5	C(C4)	2.08	0.25	0.12	10(28.4) 15(35.2) 19(26.7)
6	C(C5)	2.08	0.26	0.12	11(27.5) 17(35.5) 19(27.8)
7	C(O2)	2.1	0.34	0.16	16(21.9) 18(38.3) 20(34.8)
8	V(H1,C2)	2.11	0.63	0.3	9(29.8) 15(44.3)
9	V(H2,C2)	2.12	0.66	0.31	3(10.7) 8(28.3) 15(41.6)
10	V(H3,C4)	2.11	0.62	0.29	5(11.6) 15(41.1) 19(27.5)
11	V(H4,C5)	2.09	0.67	0.32	6(10.6) 17(44.5) 19(25.2)
12	V(O1)	4.42	1.42	0.32	1(15.2) 13(65.2) 14(13.8)
13	V(O1,C1)	3.08	1.43	0.46	1(8.0) 2(5.9) 12(64.8) 14(18.0)
14	V(C1,C3)	2.43	1.07	0.44	2(9.3) 12(18.2) 13(24.0) 15(7.0) 16(6.4) 17(16.0)
15	V(C2,C4)	3.29	1.43	0.43	3(6.6) 5(6.3) 8(19.5) 9(19.3) 10(17.9) 14(5.3) 19(16.6)
16	V(C3,O2)	2.43	1.31	0.54	4(5.8) 7(5.7) 14(5.2) 17(15.3) 18(32.8) 20(31.7)
17	V(C3,C5)	3.5	1.5	0.43	4(6.9) 6(6.1) 11(19.9) 14(11.5) 16(13.5) 19(19.2) 20(5.0)
18	V(O2)	2.79	1.25	0.45	7(10.6) 16(34.5) 17(5.6) 20(42.0)
19	V(C4,C5)	2.35	1.14	0.48	5(6.0) 6(6.3) 10(15.1) 11(14.8) 15(20.9) 17(25.3)
20	V(O2)	2.51	1.21	0.48	7(9.9) 16(34.3) 17(6.1) 18(43.0)
21	V(C5)	0.14	0.13	0.94	11(21.0) 17(38.2) 19(21.4)

electronic rearrangement involved through the C1–C3–C2 line of bonding. Notice that one of the V(C2) basins bifurcate with the V(C1,C3) basin at the ELF=0.73, while the other one does it with the V(C2,C3) basin only at the higher ELF=0.89 value.

Decarbonylation of 3H-furan-2-one (11) via the transition state 11TS has been classified like a pericyclic reaction although there is present a single orbital disconnection on O2. The primary interaction is not a center which bears an orbital orthogonality.[11] Table VI and Fig. 7(b) reveals that two valence monosynaptic basins, V(C1)(2.34e) and V(C2)(0.09e), are associated with the C2–C1 bond breaking at the 11TS. It is clear that the V(C2) derives directly from the V(C1) basin population (55.5%). Main contributions to the V(C1) are coming from the V(C2,C3) (9.4%), and the V(H1,C2) (7.8%), and V(H2,C2) (9.4%) disynaptic valence basins. Notice that only a 5.9% of contribution arises from the V(O2,C4) basin population on the side of the C1–O2 bond which has been already broken (2.261 Å). The

TABLE VIII. Basin populations $\tilde{N}_i$, standard deviation $\sigma^2(\tilde{N}_i)$, relative fluctuation $\lambda(\tilde{N}_i)$, and main contributions of other basins $i(\%)$ to $\sigma^2(\tilde{N}_i)$ for the 15TS from the density obtained at the MP2(FC)/6-31G* level of theory.

Basin		$\tilde{N}_i$	$\sigma^2(\tilde{N}_i)$	$\lambda(\tilde{N}_i)$	Contribution analysis (%)
1	C(O1)	2.12	0.35	0.17	12(33.1) 13(61.2)
2	C(C1)	2.06	0.23	0.11	12(37.2) 13(13.1) 14(42.8)
3	C(O2)	2.1	0.34	0.16	15(18.7) 16(40.1) 17(35.0)
4	C(C2)	2.07	0.25	0.12	18(37.0) 19(22.4) 20(24.2)
5	C(C3)	2.09	0.25	0.12	10(30.2) 15(24.3) 21(29.0)
6	C(C4)	2.09	0.26	0.12	11(26.7) 18(30.3) 21(29.4) 22(5.3)
7	C(C5)	2.08	0.26	0.12	8(28.5) 9(27.8) 19(17.3) 20(21.4)
8	V(H1,C5)	2.1	0.64	0.31	7(11.5) 9(28.8) 19(22.6) 20(25.6)
9	V(H2,C5)	2.07	0.64	0.31	7(11.2) 8(28.9) 19(23.1) 20(25.8)
10	V(H3,C3)	2.14	0.58	0.27	5(13.1) 15(23.9) 16(11.6) 17(7.4) 21(31.1)
11	V(H4,C4)	2.08	0.65	0.31	6(10.6) 18(30.9) 21(31.0) 22(11.5)
12	V(O1,C1)	3.1	1.44	0.46	1(8.1) 2(5.9) 13(64.7) 14(17.5)
13	V(O1)	4.42	1.42	0.32	1(15.1) 12(65.3) 14(13.9)
14	V(C1)	2.29	0.98	0.43	2(9.9) 12(25.5) 13(20.0) 17(7.1) 18(9.2) 19(9.8)
15	V(O2,C3)	2.11	1.2	0.57	3(5.4) 5(5.1) 10(11.5) 16(32.3) 17(29.2) 21(11.8)
16	V(O2)	2.87	1.23	0.43	3(11.2) 10(5.5) 15(31.6) 17(40.7)
17	V(O2)	2.59	1.21	0.47	3(10.0) 14(5.8) 15(28.9) 16(41.2)
18	V(C2,C4)	2.86	1.31	0.46	6(6.0) 11(15.4) 14(6.9) 19(12.2) 20(13.9) 21(19.8) 21(19.8) 22(8.6)
19	V(C2,C5)	1.83	1.01	0.55	4(5.4) 8(14.4) 9(14.7) 14(9.6) 18(15.7) 20(27.5)
20	V(C2,C5)	1.94	1.01	0.52	4(5.9) 7(5.5) 8(16.2) 9(16.4) 18(17.9) 19(27.5)
21	V(C3,C4)	2.55	1.21	0.47	5(6.0) 6(6.3) 10(14.9) 11(16.7) 15(11.7) 18(21.4) 22(8.0)
22	V(C4)	0.44	0.37	0.84	11(20.2) 18(30.2) 21(26.3)

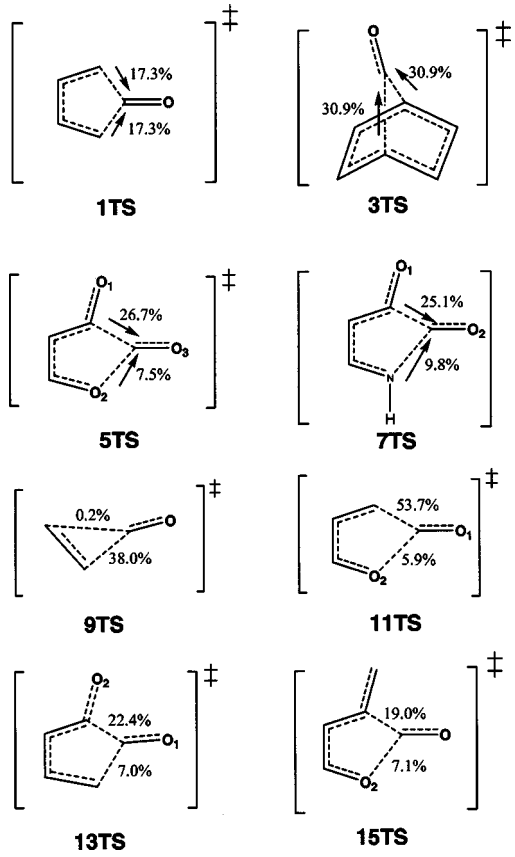

FIG. 8. Schematic view of the average bonding contributions to the ''lone pair'' region centered at the carbon atom of the CO leaving group.

corresponding bifurcation diagram in Fig. 7(b) reveals indeed the strongest correlation between the $V(\mathrm{C2,C3})$, $V(\mathrm{C3,C4})$ and the two monosynaptic $V(\mathrm{C3})$ basins which arise from the C4–C2 double bond rearrangement.

Decarbonylation of 3-cyclo-1,2-dione (13) via the transition state 13TS is a pseudopericyclic reaction.[11] Table VII and Fig. 7(c) shows a strongest bonding between the fragments at the disconnection than in the 11TS structure. The valence disynaptic $V(\mathrm{C1,C3})$ basin with $2.43e$ is being delocalized mainly with the $V(\mathrm{C3,C5})$ basin (16.0%). A fluctuation contribution of 7.0% is coming from the interaction associated with the C4–C2 bond. This pattern of bonding is also clear from the bifurcation diagram depicted in Fig. 7(c).

Decarbonylation of 3-methylene-3H-furan-2-one (15) via the transition state 15TS has been also described like a pseudopericyclic reaction with a poor match between the electrophilic and nucleophilic sites.[11] The C1–O2 bond has been early broken along the reaction coordinate, being 2.154 Å at the 15TS, while the C1–C2 bond distance is only 1.96 Å. Table VIII and Fig. 7(d) reveals that main contributions to the valence monosynaptic $V(\mathrm{C1})$ basin population $(2.29e)$, associated at the C1 extremum of the migrating CO, is effectively coming from $V(\mathrm{C2,C4})$ (9.2%) and the $V(\mathrm{C2,C5})$ (9.8%) basins. Only a 7.1% arises from the nonbonding $V(\mathrm{O2})$ basin populations. The associated bifurcation diagram involving the $V(\mathrm{C2,C4})$, $V(\mathrm{C4})$, and $V(\mathrm{C2,C3})$ basin domains in Fig. 7(d), remarks on the high delocalization associated with the electron rearrangement which participate in the formation of the new double bonds between the C2–C4 and O2–C3 centers.

IV. CONCLUDING REMARKS

A clear picture of bonding at each TS derive naturally from the fluctuation (i.e., interpreted as electron delocalization) associated with the reaction center at the departure of the CO. The ELF picture of bonding reveals clearly such a type of monosynaptic or disynaptic type of interaction. These key basins are the numbered in Tables I–VIII as 15, 16 and 17, 14, 18, 13, 13, 14, and 14 for 1TS, 3TS, 5TS, TS, 9TS, 11TS, and 15TS, respectively. Figure 8 sketches the main bonding contributions to the ''lone pair'' region centered at the carbon atom of the CO leaving group being arising from the remaining molecular fragment along both pericyclic and pseudopericyclic reactions.

ACKNOWLEDGMENTS

This work was supported by FONDECYT, Grant No. 1030173, and by Dirección de Investigación, Universidad Andrés Bello, Grant No. DI-UNAB 11-02.

[1] (a) A. R. De Lera and F. P. Cossio, Angew. Chem. Int. Ed. Engl. **41**, 1150 (2002); (b) J. Rodriguez-Otero and E. M. Cabaleiro-Lago, *ibid.* **41**, 1147 (2002).
[2] C. Zhou and D. M. Birney, J. Am. Chem. Soc. **124**, 5231 (2002).
[3] J. W. Cubbage, Y. Guo, R. D. McCulla, and W. S. Jenks, J. Org. Chem. **66**, 8722 (2001).
[4] (a) M. Alajarin, P. Sanchez-Andrada, F. P. Cossio, A. Arrieta, and B. Lecea, J. Org. Chem. **66**, 8470 (2001); (b) M. Alajarin, A. Vidal, P. Sanchez-Andrada, and F. Tovar, and G. Ochoa, Organic Lett. **2**, 965 (2000).
[5] W. W. Shumway, N. K. Dalley, and D. M. Birney, J. Org. Chem. **66**, 5832 (2001).
[6] G. Rauhut, J. Org. Chem. **66**, 5444 (2001).
[7] A. R. De Lera, R. Alavrez, B. Lecea, A. Torrado, F. P. Cossio, and F. P. Angew, Angew. Chem. Int. Ed. Engl. **40**, 557 (2001).
[8] D. M. Birney, J. Am. Chem. Soc. **122**, 10917 (2000).
[9] D. M. Birney, X. Xu, and S. Ham, Angew. Chem. Int. Ed. Engl. **38**, 189 (1999).
[10] L. Luo, M. D. Bartberger, and W. R. Dolbier, Jr., J. Am. Chem. Soc. **119**, 12366 (1997).
[11] D. M. Birney, S. Ham, and G. R. Unrut, J. Am. Chem. Soc. **119**, 4509 (1997).
[12] R. B. Woodward and R. Hoffmann, *The Conservation of Orbital Symmetry* (Chemie, Weinheim, 1970).
[13] R. F. Bader, *Atoms in Molecules: A Quantum Theory* (Oxford University Press, Oxford, 1994).
[14] (a) A. Savin, R. Nesper, S. Wengert, and T. F. Fäsler, Angew. Chem. Int. Ed. Engl. **36**, 1808 (1997); (b) D. Max and A. Savin, *ibid.* **36**, 2077 (1997); (c) A. Savin, A. D. Becke, J. Flad, R. Nesper, H. Preuss, and H. von Schnering, *ibid.* **30**, 409 (1991).
[15] A. D. Becke and K. E. Edgencombe, J. Chem. Phys. **92**, 5397 (1990).
[16] (a) E. Chamorro, J. C. Santos, B. Gómez, R. Contreras, and P. Fuentealba, J. Chem. Phys. **114**, 23 (2001); (b) J. Phys. Chem. A **106**, 11533 (2002).
[17] (a) B. Silvi and A. Savin, Nature (London) **371**, 683 (1994); (b) A. Savin, B. Silvi, and F. Colonna, Can. J. Chem. **74**, 1088 (1996); (c) S. Noury, F. Colonna, and A. Savin, J. Mol. Struct. **450**, 59 (1997).
[18] For recent applications see, for instance: (a) O. Hochrein, M. Kohout, W. Schnelle, and R. Kniep, Z. Anorg. Allg. Chem. **628**, 2738 (2002); (b) R. J. Gillespie and B. Silvi, Coord. Chem. Rev. **233**, 53 (2002); (c) S. Berski and Z. Latajka, Int. J. Quantum Chem. **90**, 1108 (2002); (d) G. Frison and A. Sevin, J. Chem. Soc., Perkin Trans. 2 **10**, 1692 (2002); (e) F. Zurcher and R. Nesper, Z. Anorg. Allg. Chem. **628**, 1581 (2002); (f) D. B. Chesnut and L. Bartolotti, J. Chem. Phys. **278**, 101 (2002); (g) E. Chamorro, A. Toro-Labbe, and P. Fuentealba, J. Phys. Chem. A **106**, 3891 (2002); (h) S. Noury, B. Silvi, and R. J. Gillespie, Inorg. Chem. **41**, 2164 (2002).
[19] R. F. W. Bader, *Localization and Delocalization in Quantum Chemistry*,

edited by O. Chalvet *et al.* (Reidel, Dordrecht, 1976), Vol. 1.
[20] For details concerning several applications both in the AIM and ELF schemes see for instance: (a) X. Fradera, J. Poater, S. Simon, M. Duran, and M. Sola, Theor. Chem. Acc. **108**, 214 (2002); (b) J. Poater, M. Sola, M. Duran, and X. Fradera, *ibid.* **107**, 362 (2002); (c) X. Fradera and M. Sola, J. Comput. Chem. **23**, 1347 (2002); (d) D. B. Chesnut and L. Bartolotti, J. Chem. Phys. **257**, 175 (2000); (e) I. Fourré, B. Silvi, P. Chaquin, and A. Sevin, J. Comput. Chem. **20**, 897 (1999); (f) X. Fradera, M. A. Austen, and R. F. W. Bader, J. Phys. Chem. A **103**, 304 (1999); (g) R. Llusar, A. Beltrán, J. Andrés, S. Noury, and B. Silvi, J. Comput. Chem. **20**, 1517 (1999).
[21] M. J. Frisch, G. W. Trucks, H. B. Schlegel *et al.* Revision A.9, GAUSSIAN 98, Gaussian, Inc., Pittsburgh, PA, 1998.
[22] S. Noury, X. Krokidis, F. Fuster, and B. Silvi, TOPMOD package, Universite Pierre et Marie Curie, 1997.
[23] S. Noury, X. Krokidis, F. Fuster, and B. Silvi, Comput. Chem. (Oxford) **23**, 597 (1999).
[24] (a) B. Hibbard, J. Kellum, and B. Paul, VIS5D 5.1, Visualization Project. University of Winconsin-Madison Space Science and Engineering Center (SSEC); (b) W. L. Hibbard and D. Santek, Proc. IEEE **129**, 28 (1990).
[25] J. K. Burdett and T. A. McCormick, J. Phys. Chem. A **102**, 6366 (1998).